ARTICLES

Evaporation of Ethanol and Ethanol−Water Mixtures Studied by Time-Resolved Infrared Spectroscopy

Plinio Innocenzi,* Luca Malfatti, Stefano Costacurta, and Tongjit Kidchob

Laboratorio di Scienza dei Materiali e Nanotecnologie, D.A.P., Università di Sassari, and CR-INSTM, Palazzo del Pou Salid, Piazza Duomo 6, 07041 Alghero (Sassari), Italy

Massimo Piccinini and Augusto Marcelli

Laboratori Nazionali di Frascati - INFN, Via E. Fermi 40, 00044, Frascati, Italy

Received: November 23, 2007; Revised Manuscript Received: April 29, 2008

The knowledge of the physics and the chemistry behind the evaporation of solvents is very important for the development of several technologies, especially in the fabrication of thin films from liquid phase and the organization of nanostructures by evaporation-induced self-assembly. Ethanol, in particular, is one of the most common solvents in sol−gel and evaporation-induced self-assembly processing of thin films, and a detailed understanding of its role during these processes is of fundamental importance. Rapid scan time-resolved infrared spectroscopy has been applied to study in situ the evaporation of ethanol and ethanol-water droplets on a ZnSe substrate. Whereas the evaporation rate of ethanol remains constant during the process, water is adsorbed by the ethanol droplet from the external environment and evaporates in three stages that are characterized by different evaporation rates. The adsorption and evaporation process of water in an ethanol droplet has been observed to follow a complex behavior: due to this reason, it has been analyzed by two-dimensional infrared correlation. Three different components in the water bending band have been resolved.

Introduction

Deposition of thin films from the liquid phase is a widely used technology for fabrication of coating layers of oxides, organic polymers and hybrid organic−inorganic materials. Thin films are generally deposited by dip-coating, spin-coating and spray-coating in controlled conditions, i.e., temperature, pressure and relative humidity in the deposition room. Sol−gel processing is a typical example of technology for film deposition by liquid phase and several products are now on the market, such as antireflective and antiscratch coatings.[1,2] Self-assembly through supramolecular organic templates is another method to deposit thin films from the liquid phase that allows production of mesoporous films;[3] these films show an organized porosity at the mesoscale (2−50 nm) after removal of the template. At the basis of the mesoporous films processing there is evaporation-induced self-assembly (EISA), in which solvent evaporation induces self-organization of the micelles. EISA is also used to drive self-organization of nanoparticles or bacteria in ordered structures.[4,5] In all these examples, from sol−gel to EISA processing, the evaporation of the solvent plays a crucial role. A deep knowledge of this very basic phenomenon is, therefore, fundamental for a real understanding and control of film deposition via the liquid phase.

In sol−gel and EISA deposition techniques, ethanol is the most widely used solvent, which is often preferred to methanol due to its lower toxicity and due to lower vapor pressure with respect to other alcohols. A typical sol−gel reaction involves an alkoxide, a solvent (typically an alcohol ensuring homogeneity and water for hydrolysis) and an acid or a base as the catalyst. Sol−gel is also at the basis of EISA processing of mesoporous thin films: in such a case the role of solvent is critical because it is only during the evaporation phase that the critical micelle concentration is reached and self-organization of the template occurs. In previous studies, multistep evaporation rates, attributed to water uptaking, have already been observed by interferometry for sol−gel film deposition.[6] Controlling water and ethanol evaporation is, therefore, necessary during thin film deposition.

It is not surprising that, even nowadays, there is a lack on available data about simple yet extremely important features of the physics and the chemistry behind basic phenomena. Studies on ethanol evaporation, water and binary water−ethanol mixtures have been already performed on different surfaces by studying the changes in the contact angle.[7,8] The evaporation of an ethanol−water aerosol droplet has been also followed by cavity enhanced Raman scattering and laser induced fluorescence,[9] whereas fluorescence spectroscopy has been used to probe the evolving size of evaporating droplets.[10] Experiments on droplet evaporation on solid surfaces have shown that two pure modes of evaporation can be identified:[11] one consists of the decrease of the drop−substrate contact area maintaining the contact angle constant, and the second mode results in the decrease of the contact angle keeping the surface area constant. Phenomenologically, the evaporation process can follow either a pure mode or a mixed type, where the mode changes in the

---

* Corresponding author. E-mail: plinio@uniss.it.

10.1021/jp7111395 CCC: $40.75

course of evaporation.[11,12] Details on the solvent evaporation process appear, however, still to be fully disclosed.[13]

In previous works, to investigate time-resolved phenomena during self-assembly of mesoporous thin films (the reactions and the evaporation rates of the different components), we have applied time-dependent and time-resolved infrared techniques.[14] In particular,[15] we have observed that in situ rapid scan infrared spectroscopy is very suitable for monitoring solvent and water evaporation during film deposition. Because of the complexity of the system, however, not all the details of the process could be fully explained. It appears, instead, that some phenomena have been somehow neglected. We have, therefore, recognized the need for a very basic comprehension of the evaporation processes related to ethanol at ambient conditions; this is the simplest and likely the most important system for driving self-assembly phenomena and sol−gel reactions. In the present work, rapid scan infrared spectroscopy has been applied to investigate the evaporation of ethanol droplets cast on an infrared transparent substrate and two-dimensional (2D) correlation has been used to analyze the data.[16–18]

Experimental Section

Ethanol (EtOH) anhydrous (RPE) for analysis, water content <0.1%, and double-distilled water were used for the evaporation experiments; ethanol was purchased from Carlo Erba Reagents and used without further purification.

Time-resolved in situ infrared (IR) analysis was performed at the synchrotron infrared beamline (SINBAD) at the Laboratori Nazionali di Frascati (Frascati, Italy) of the Istituto Nazionale di Fisica Nucleare (INFN) using a Bruker Equinox 55; a conventional Globar source was used. The IR measurements were performed using the interferometer working in vacuum, in the range 600−4000 cm^{-1} and with a resolution of 8 cm^{-1}. A MCT detector (1 mm^2 size) cooled to the nitrogen temperature and a KBr beam splitter were used. Rapid scan time-resolved (RSTR) measurements were performed by a single scan per spectrum and an acquisition time of 133 ms followed by an interval of 160 ms before the beginning of the next acquisition to study the evaporation of a cast droplet of pure ethanol and ethanol-water mixtures. We have recorded the infrared spectra in the shortest time sequence that could be achieved; the scan time used in the experiment is the best compromise in terms of signal-to-noise ratio and resolution. Another experimental parameter that we have optimized is the ethanol droplet size; if the ethanol drop is too large, the infrared signal will be saturated for most of the measurement time, on the other hand, smaller droplets show a very fast evaporation and are not suitable for time-resolved studies. The experimental conditions that we have selected are optimized for an evaluation of the physical changes of the system but do not allow us to extract quantitative data, for example, about the evaporation rate. The main reason is the high ethanol−substrate wettability; due to the low contact angle ($\theta = 30°$), the ethanol droplet quickly spreads on the substrate and only part of the droplet can be illuminated by the IR microscope. We have repeated the experiment for several runs (up to ten for each composition) to ensure reproducibility of the experimental conditions, and the experimental trend has been always the same; on the contrary, the time scale has been more difficult to reproduce due to the reasons we have previously pointed out.

The relative humidity (RH %) during the experiment was carefully monitored, and a cabinet was built around the microscope to control the RH, which was constant at 50%. The measurements were done at 25 °C and at room pressure.

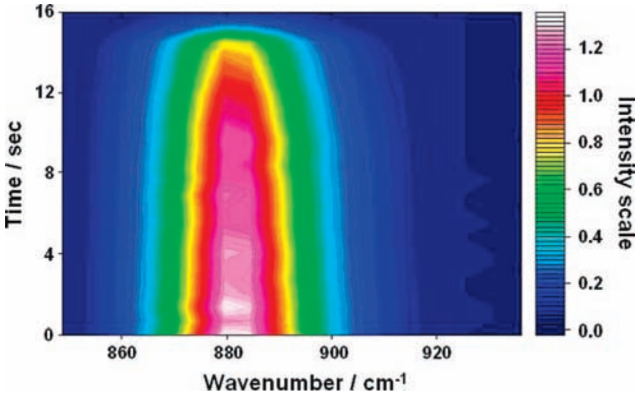

Figure 1. Three-dimensional FTIR image in the 850−930 cm^{-1} range obtained during the evaporation of a cast droplet of ethanol. The image was recorded in rapid scan time-resolved acquisition mode.

The experiments were conducted in transmission configuration, using a double-sided, forward-backward acquisition mode, with a Bruker IR microscope. The background was recorded as the average of 40 scans in air with the ZnSe substrate. In a typical experiment, a small drop of ethanol or water-ethanol mixture (50 μL) was cast on the ZnSe substrate and the measurement was started immediately afterwards. The results were analyzed by Bruker Opus 6 Software. Baseline was calculated by rubberband correction using 64 points in a range from 1840 to 1600 cm^{-1} for the bands at 1740 and 1640 cm^{-1}, and in a range from 950 to 750 cm^{-1} for the band at 880 cm^{-1}.

Results and Discussion

To monitor the evaporation process of ethanol and ethanol−water binary mixtures, we have selected specific bands attributed to the two components. This choice was dictated by the need to have a vibrational mode that is not saturated during the measurement and not overlapped to other bands. In particular, we have selected the bands at 880 cm^{-1} ν_s(C−C + C−O) and at 1760 cm^{-1} (first overtone of the band at 880 cm^{-1}) for ethanol[19,20] and the band at 1640 cm^{-1} for water (bending mode) and followed their evolution with time. The choice of the bands (see Experimental Section for details) has allowed us to obtain unsaturated signals during the overall evaporation process (see Supporting Information). In general, the choice of the bending mode of water is not the best one to follow the different components (given by different strength of the hydrogen bonds); the wider stretching band at higher energy (around 3300 cm^{-1}) allows a better separation. In the present case the saturation of the water stretching bands observed even at low water contents in the ethanol−water mixtures has restricted the choice to the water bending mode at 1640 cm^{-1}.

Figure 1 shows the three-dimensional (3D) time-resolved infrared spectra of an evaporating droplet of ethanol cast on the ZnSe substrate; the time evolution of the band at 880 cm^{-1} is shown. The *x*-axis represents the wavenumber, the *y*-axis the time scale in seconds and the different colors the intensity scale. From this image the evaporation of ethanol appears as a continuous process, the same evaporation rate[21] is observed during all the experiment. We have also analyzed the 1850−1580 cm^{-1} region in detail; the water bending mode (≈1640 cm^{-1}) and the ethanol first overtone of 880 cm^{-1} band fall in this interval. Traces of water are present even in pure ethanol whereas more water might be adsorbed from the external environment during the evaporation process. The bending mode of water is, indeed, clearly observed and it appears to have a

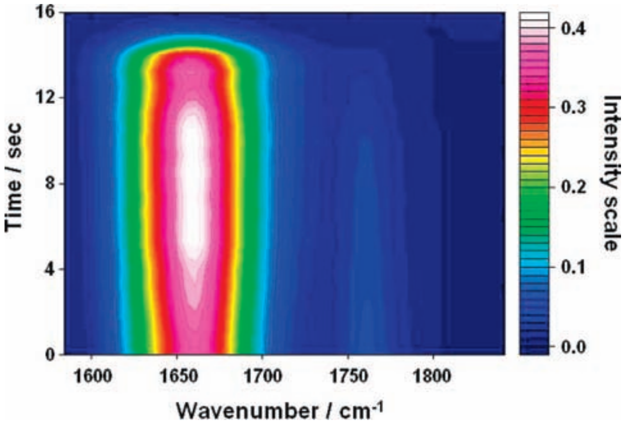

Figure 2. Three-dimensional FTIR image in the 1580−1850 cm^{-1} range obtained during the evaporation of a cast droplet of ethanol. The image was recorded in rapid scan time-resolved acquisition mode.

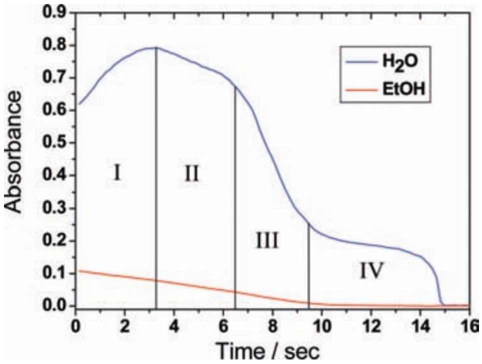

Figure 3. Changes in absorbance of water (~1660 cm^{-1}), blue line, and ethanol (~1760 cm^{-1}), red line, bands as a function of evaporation time.

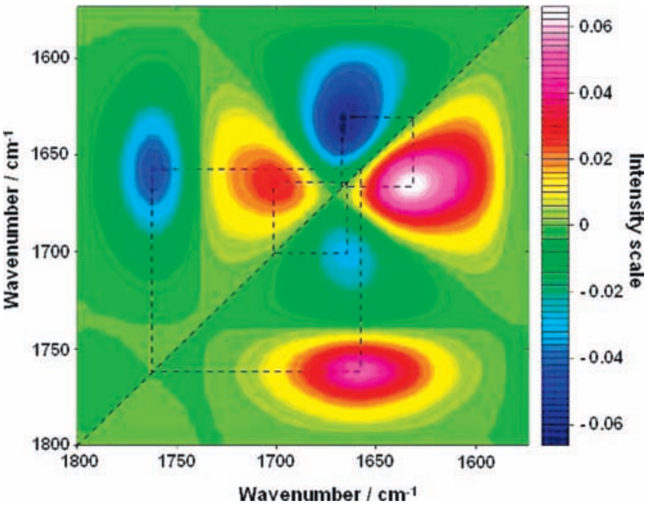

Figure 4. Asynchronous two-dimensional infrared correlation plot in the 1800−1580 cm^{-1} range of an ethanol evaporating droplet.

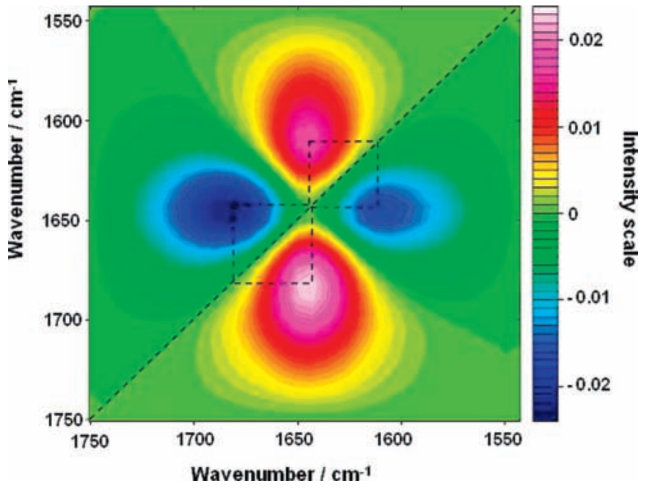

Figure 5. Asynchronous two-dimensional infrared correlation plot in the 1800−1540 cm^{-1} range of an evaporating droplet of pure water. The 2D spectra have been obtained taking the water spectra relative to the last stage of evaporation.

much more complex time-dependent behavior than ethanol, which shows a constant evaporation rate. Figure 2 shows the 3D time-resolved infrared spectra of water in the ethanol evaporating droplet, a maximum can be clearly observed. We have reported in a separate graph the changes in absorbance of the peak of the water and ethanol bands as a function of the evaporation time (Figure 3). As we have observed in the 3D time-resolved spectra, the evaporation of ethanol is continuous with a constant evaporation rate, whilst the spectra of water as a function of time are the result of a complex absorption-evaporation process. We have identified four different trends for water: (I) a first stage during which water is adsorbed by ethanol from the external environment, this process reaches a maximum after few seconds from the beginning of the evaporation. It is interesting to observe that the water content in the evaporating droplet increases even if ethanol continuously decreases. (II) Water, after reaching a maximum, starts to evaporate: this is indicated by a decrease of the curve intensity. (III) The curve shows a drastic change of the slope and after this point, which is at around half of the process, the evaporation is very fast. This stage corresponds to the last part of ethanol evaporation. (IV) Ethanol is completely evaporated; the small residual droplet is now composed only of water, which eventually evaporates in a few seconds. We can also observe, from the simultaneous evolution of water and ethanol intensities, that even if water exhibits a complex behavior, which is evidenced by four different evaporation stages, this does not affect the ethanol evaporation rate, which remains constant.

The results on ethanol evaporation are in good agreement with previous findings: experiments conducted by studying the evaporation rate and the drop profile of pure ethanol have shown that there is a monotonic evolution with time.[7] These experiments, however, do not take into account the possible presence of water, which can be observed only by using time-resolved infrared spectroscopy.

We can also analyze more in detail the evolution of the water band by using 2D correlation infrared analysis,[22] this method has revealed to be very effective to study the water structure.[18] We have built the asynchronous spectra in the 1800−1540 cm^{-1} interval. An average spectrum was used as the reference for the analysis of the 2D spectra. Figure 4 shows the asynchronous 2D spectra of an evaporating water droplet, three correlation squares can be built;[22] the correlation spectra have been obtained by extracting the FTIR spectra corresponding to the evaporation steps (stages from II to IV in Figure 3). One of the advantages of 2D analysis is the improved resolution that can be achieved, in this case we can identify four different species that respond to the change of the external variable (in this case, time). Three of these bands are attributed to water (1630, 1670, 1720 cm^{-1})[23,24] and the fourth one to ethanol (1760 cm^{-1}). The water network structure is generally described by a simple model, which is based on three levels of connectivity.[25] Gaussian fitting of the wide stretching band around 3300 cm^{-1} gives three

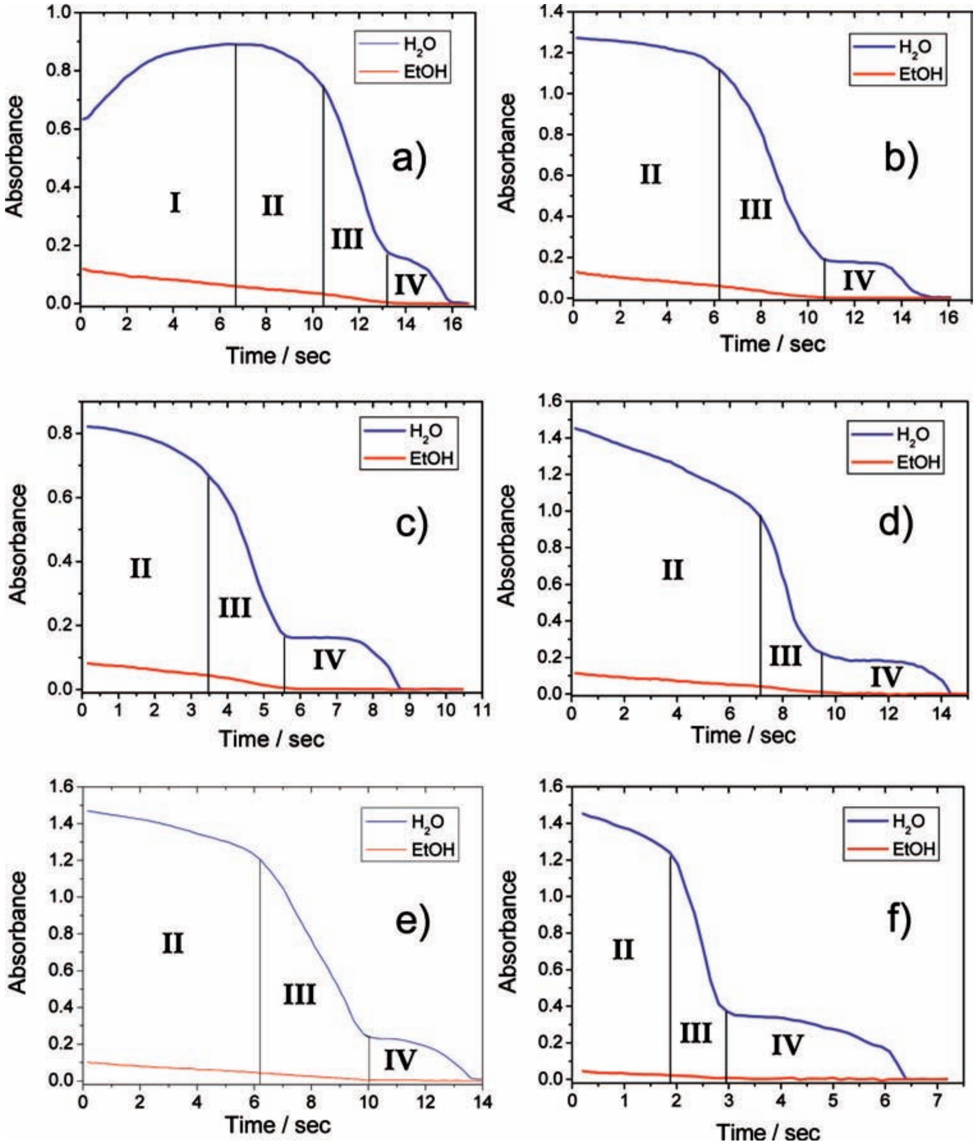

Figure 6. Changes in absorbance of water (≈1660 cm^{-1}), blue line, and ethanol (≈1760 cm^{-1}), red line, bands as a function of evaporation time for six different concentrations (from 99 (a), to 94 (f) vol % of ethanol) of ethanol−water binary mixtures.

components that are assigned to "*network water*" (~3320 cm^{-1}), "*intermediate water*" (~3465 cm^{-1}) and "*multimer water*" (~3585 cm^{-1}).[26] The bending mode (around 1650 cm^{-1}) of water is much more narrow and much less sensitive to changes of the network structure; identification of the different components on the basis of the literature is also difficult because of the lack of systematic data. Previous studies of water confinement in micellar systems have, however, allowed us to identify at least two Gaussian components at ~1625 and ~1660 cm^{-1}, which have been attributed to "*intermediate water*" and "*network water*", respectively.[24,27] 2D correlation spectra suggest, in the present case, the presence of three correlated components. On the other hand, also the fitting that we have performed using the water bending bands obtained from the time-resolved analysis, is achieved by using three Gaussian components. We attribute the three bands that we have resolved in the bending mode of water by Gaussian fitting and the correlated peaks from 2D correlation analysis to "*multimer water*" (1630 cm^{-1}), "*intermediate water*" (1670 cm^{-1}) and "*network water*" (1720 cm^{-1}), in accordance with the simple model for water structure.

The correlation squares in 2D correlation spectra show that there is an asynchronous correlation between ethanol and *intermediate water*: the two bands respond to the time change but one increases in intensity while the other shows a simultaneous decrease. In addition, there are other asynchronous correlations: *intermediate water*-*multimer water* and *intermediate water*-*network water*. To interpret these 2D data, we have to keep in mind that the water bands have a complex evolution with time: they increase and decrease in intensity and do not have a monotonic trend; furthermore small overlapping of the bands are present and this can be also a source of error (see Supporting Information, where full spectra in the last evaporation seconds are shown). In particular, overlapping of the ethanol first overtone with the bending mode of water and overlapping of water with the tail of the δ_a(HCH) band of ethanol are observed. The different correlation peaks shown by the 2D correlation spectra could be, therefore, originated by the overlapping of these bands. To clarify this point, we have performed similar experiments of evaporation with pure water. In this case the FTIR time rapid scan experiments are very difficult to perform in the middle infrared range because even the signal from the bending band is easily saturated. We were able, however, to record good signals from the last stage of the water evaporation and we have used these data to obtain a 2D asynchronous spectrum of evaporating water in the 1550−1750 cm^{-1} range (Figure 5). In this case ethanol overlapping can be discarded and we still observed three components for evaporating water, which we can attribute to the presence of the different correlated components in the bending mode of water. The complex evaporation process shown by water is likely correlated with the presence of different water species; adsorbed water appears to be the main responsible for the first and second stage, whereas the other components mostly evaporate during stages III and IV.

We have extended the time-resolved rapid scan experiments to water−ethanol mixtures. Controlled amounts of water have been added to pure ethanol to obtain binary mixtures, in the 1−10 vol % of water in ethanol. This interval has been selected taking into account the azeotrope of the ethanol−water mixture, which is at the liquid composition of 95.5% in ethanol and 4.5% water, percentage by weight.[28] We have, therefore, monitored the evaporation of mixed compositions close to the azeotrope. Figure 6 (parts a−f) shows the evolution of water and ethanol peak intensity with evaporation time; the results show that in all of the ethanol−water mixtures, the ethanol evaporation rate remains constant, as in the case of pure ethanol. With the increase of water content, however, there is a change in the different evaporation stages, whereas four stages are still observed in the 99 EtOH−1 H_2O composition, in the other compositions only three stages are detected. It must be observed that in the compositions in which the water content is higher than 1 vol %, the signal of the bending mode of water results saturated at the beginning of the evaporation. It is difficult, therefore, to state whether at higher water contents the first stage of water adsorption occurs or not.

Conclusions

Rapid scan time-resolved infrared spectroscopy has shown to be an important tool to study the evaporation process of alcohols, in particular, ethanol. Details of the process can be disclosed with a good time resolution, which is difficult to achieve using other techniques.

The evaporation of a cast drop of ethanol has shown that the adsorption of water must be taken into account for a better understanding of the process. The first stage of the phenomenon is dominated by the adsorption of water. The following evaporation of water occurs in three different stages characterized by different rates. On the other hand, ethanol evaporation exhibits a monotonic trend that is not affected by the complex behavior of water. If low amounts of water are added to ethanol, the tendency is the same. The multistage behavior exhibited by water during evaporation is likely related to the different water components, as shown by 2D correlation analysis.

Acknowledgment. This research was supported by the Italian Ministero dell'Università e della Ricerca (MiUR) through FIRB2001 (RBNE01P4JF) and FIRB2003 (RBNE033KMA) and PRIN grants.

Supporting Information Available: FTIR spectra. This material is available free of charge via the Internet at http://pubs.acs.org.

References and Notes

(1) Ashley, C. S.; Reed, S. T. Sol-gel antireflective coating on plastics, United States Patent 4929278, 1990.

(2) Hofacker, S.; Mechtel, M.; Magerb, M.; Kraus, H. *Prog. Org. Coat.* **2002**, *45*, 159.

(3) Brinker, C.J.; Lu, Y.; Sellinger, A.; Fan, H. *Adv. Mater.* **1999**, *11*, 579. (a) Soler-Illia, G.; Sanchez, C.; Lebeau, B.; Patarin, J. *Chem. Rev* **2002**, *102*, 4093. (b) Antonietti, M.; Ozin, G. A. *Chem. Eur. J.* **2004**, *10*, 28. (c) Soler-Illia, G.; Innocenzi, P. *Chem. Eur. J.* **2006**, *12*, 4478.

(4) Shevchenko, E. V.; Talapin, D. V.; Kotov, N. A.; O'Brien, S.; Murray, C. B. *Nature* **2006**, *439*, 55.

(5) Nellimoottil, T. T.; Rao, P. N.; Ghosh, S. S.; Chattopadhyay, A. *Langmuir* **2007**, *23*, 8655.

(6) (a) Grosso, D.; Cagnol, F.; Soler-Illia, G.J.; Crepaldi, E. L.; Amenitsch, H.; Brunet-Bruneau, A.; Bourgeois, A.; Sanchez, C. *Adv. Funct. Mater.* **2004**, *14*, 309. (b) Grosso, D.; Babonneau, F.; Albouy, P.A.; Amenitsch, H.; Balkenende, A.R.; Brunet-Bruneau, A.; Rivory, J. *Chem. Mater.* **2002**, *14*, 931.

(7) Sefiane, K.; Tadrist, L.; Douglas, M. *Int.J.Heat Mass Transf.* **2003**, *46*, 4527.

(8) Cheng, A.; Sefiane, K. H.; Soolaman, D.; Tadrist, L.; Douglas, M.; Yu, H. Z. *Int. J. Phys. Chem. B* **2006**, *110*, 11267.

(9) Hopkins, R. J.; Reid, J. P. *J. Phys. Chem. A* **2005**, *109*, 7923.

(10) Tzeng, H. M.; Wall, K. F.; Long, M. B.; Chang, R. K. *Opt. Lett.* **1984**, *9*, 273.

(11) Erbil, H. Y.; McHale, G.; Newton, M. I. *Langmuir* **2002**, *18*, 2636.

(12) Lam, C. N.; Wu, R.; Li, D.; Hair, M.L.; Neumann, A.W. *Adv. Colloid Interf. Sci.* **2002**, *96*, 169.

(13) Fang, X.; Li, B.; Petersen, E.; Ji, Y.; Sokolov, J. C.; Rafailovich, M. H. *J. Phys. Chem. B* **2005**, *109*, 20554.

(14) (a) Innocenzi, P.; Malfatti, L.; Kidchob, T.; Falcaro, P.; Cestelli.Guidi, M.; Piccinini, M.; Marcelli, A. *Chem.Commun.* **2005**, 2385. (b) Falcaro, P.; Costacurta, S.; Mattei, G.; Amenitsch, H.; Marcelli, A.; Cestelli Guidi, M.; Piccinini, M.; Nucara, A.; Malfatti, L.; Kidchob, T.; Innocenzi, P. *J. Am. Chem. Soc.* **2005**, *127*, 3838. (c) Innocenzi, P.; Kidchob, T.; Mio Bertolo, J.; Piccinini, M.; Cestelli Guidi, M.; Marcelli, A. *J. Phys. Chem. B* **2006**, *110*, 10837.

(15) Innocenzi, P.; Malfatti, L.; Kidchob, T.; Costacurta, S.; Falcaro, P.; Piccinini, M.; Marcelli, A.; Morini, P.; Sali, D.; Amenitsch, H. *J. Phys. Chem. C* **2007**, *111*, 5345.

(16) Noda, I. *Vibr. Spectrosc.* **2004**, *36*, 143.

(17) Noda, I.; Dowrey, A. E.; Marcott, C.; Story, G. M.; Ozaki, Y. *Appl. Spectrosc.* **2000**, *54*, 236A.

(18) Segtnan, V. H.; Sasic, S.; Isaksson, T.; Ozaki, Y. *Anal.Chem.* **2001**, *73*, 3153.

(19) Plyler, E. K. *J. Res. Nat. Bureau Stand.* **1952**, *48*, 281.

(20) Innocenzi, P. *J. Non-Cryst. Solids* **2003**, *316*, 309.

(21) We have used the term "evaporation rate" to indicate the d*I*/d*t*, the rate of intensity change with time.

(22) Noda, I.; Ozaki, Y. *Two-Dimensional Correlation Spectroscopy - Applications in Vibrational and Optical Spectroscopy*, John Wiley & Sons: Chichester, England, 2003.

(23) Buch, V., Devlin, J. P., Eds. *Water in Confining Geometries*; Springer,: New York, 2003.

(24) Boissiere, C.; Brubach, J.B.; Marmet, A.; De Marzi, G.; Bourgaux, C.; Prouzet, E.; Roy, P. *J. Phys. Chem. B* **2002**, *106*, 1032.

(25) Czarnik-Matusewicz, B.; Pilorz, S.; Hawranek, J. P. *Anal. Chim. Acta* **2005**, *544*, 15.

(26) Brubach, J.-B.; Mermet, A.; Filabozzi, A.; Gerschel, A.; Roy, P. *J. Chem. Phys.* **2005**, *122*, 184509.

(27) Brubach, J.-B.; Mermet, A.; Filabozzi, A.; Gerschel, A.; Lairez, D.; Krafft, M.P.; Roy, P. *J. Chem. Phys.* **2001**, *105*, 430.

(28) Lide, D. R., Ed. CRC-Handbook of Chemistry and Physics, 87th ed.; Taylar and Francis: Boca Raton, FL, 2007; http://www.hbcpnetbase.com; pp 6−157.

JP7111395